Performance Studies of Multiband Square Patch Log-Periodic Antennas

Original Scientific Paper

Gilang Arya Nur Fauzan
Universitas Negeri Surabaya, Faculty of Engineering,
Department of Electrical Engineering,
Surabaya, Indonesia
gilang.22080@mhs.unesa.ac.id

Nurhayati Nurhayati*
Universitas Negeri Surabaya, Faculty of Engineering,
Department of Electrical Engineering,
Surabaya, Indonesia
nurhayati@unesa.ac.id

L Endah Cahya Ningrum
Universitas Negeri Surabaya, Faculty of Engineering,
Department of Electrical Engineering,
Surabaya, Indonesia
endahningrum@unesa.ac.id

*Corresponding author

Atul Varshney
Graphic Era (Deemed to be University),
ECE Department, FET,
Dehradun 248002, Uttarakhand, India
atul.varshney@gkv.ac.in

Raimundo Eider Figueredo
Technological Federal University of Paraná (UTFPR),
Brazil
raimundoeider@alunos.utfpr.edu.br

Abstract *– Rapid technological developments demand compact, lightweight, and high-performance wireless communication components, necessitating efforts to optimize multiband antenna technology that ensures affordable access across a wide range of modern applications. Multiband antennas can operate at several different frequencies in a variety of applications, reducing the number of antennas used, saving space and costs. This study compares five models of microstrip Log-Periodic Antenna (LPA) using modified rectangular geometry, namely model 1 (U-shaped), model 2 (S-shaped), model 3 (O-shaped), model 4 (full rectangle), and model 5 (rhombus-shaped). The five antennas were constructed with identical substrate dimensions, differing just in the configuration of the patch radiator, and were simulated using a full-wave electromagnetic solver (CST Studio Suite) at a frequency range of 3-11 GHz, utilizing a dual-layer Rogers RO4003C substrate to enhance radiation efficiency and stability. Analysis is carried out on parameters such as return loss, surface current, radiation pattern, and directivity. Antenna models 1 to 5 produce 4,7,5,5, and 8 different Multiband frequencies. Model 5 provides eight resonance frequencies at 2.4, 3.0, 3.7, 5.7, 7.6, 10.0, 10.5, and 10.9 GHz, with a minimum reflection coefficient of –37.86 dB at 5.7 GHz and a peak directivity of 9.21 dBi at 4 GHz. Additionally, the results of measurement and simulation of the Model 5 were compared, with some fulfilling the specified criteria. The findings indicated that all five antennas are capable of functioning at multiband frequencies, rendering them appropriate for diverse communication technologies and applications such as, IoT, UAVs, radar, and others.*

Keywords*: gain antenna, Log-periodic antenna, microstrip, multiband, UAV*

Received: October 11, 2025; Received in revised form: December 13, 2025; Accepted: December 23, 2025

1. INTRODUCTION

The rapid evolution of communication and radar technology has intensified the need for compact, lightweight, and high-performance wireless communication components. Antennas, as critical elements for data transmission, must satisfy physical constraints while delivering stable multiband operation across dynamic environments [1]. Multiband antennas can be used in mobile devices to support multiple wireless technologies for applications such as: Radio communications (VHF, UHF), Satellite communications (C-band, Ku-band, Ka-band). They can be used in Internet of Things (IoT) devices to support multiple wireless tech-

nologies, such as Wi-Fi, Bluetooth, and Zigbee. 5G [2] and LoRaWAN [3, 4]. Multiband antennas can also be used to support communication between unmanned aerial vehicles (UAVs) and ground control stations on several different frequencies, such as: L-band (1-2 GHz), S-band (2-4 GHz), C-band (4-8 GHz), X-band (8-12 GHz) [5-9]. Multiband antennas are also used in UAV radar systems to detect and track targets on several different frequencies in the Ku-band (12-18 GHz) and Ka-band (26.5-40 GHz)[10-12].

Furthermore, multiband antennas are used to support UAV navigation by receiving signals from several navigation systems, such as: Global Positioning System (GPS) on sub-bands L1: 1575 MHz, L2: 1227 MHz, Global Navigation Satellite System (GLONASS) within frequencies L1: 1602 MHz, L2: 1246 MHz) and UAV satellite communications on several different frequencies, as well as in UAV remote sensing systems to detect and analyze data on several different frequencies in the L, S, and C bands. Thus, multiband antennas can improve performance and flexibility, including UAV and airborne technologies and various communications, radar, surveying, monitoring, and remote sensing applications [13-15].

The antenna is a crucial component that must be adjusted to fulfill the requirements of wireless standards for application sharing, as it serves as the front end of communications and radar systems. Diverse methodologies have been established to enhance antenna efficacy and achieve multiband frequency performance, including reconfigurable techniques utilizing external components or incorporating supplementary structures. In antenna design, substrate selection plays a critical role. Rogers RO4003C substrate material has advantages at higher frequencies compared to FR4. Its superior dielectric characteristics and low loss make it a preferred substrate for designing multiband antennas across a wide frequency range. Enhancements such as slot-loading, parasitic stubs, and fractal patterns have further improved impedance matching and radiation properties.

Many researchers have designed antennas that can work at multi-band frequencies, including antenna designs that use flexible materials that can work at terahertz frequencies [16]. The antenna is small in size because it operates at terahertz frequencies, and produces two frequency band at 123 GHz and 180 GHz. A distinct multiband antenna design at terahertz frequencies has been achieved [17] by generating two multiband frequencies at 9.53 GHz and 24.19 GHz, at 0.6 and 0.7 THz [18], and at 0.65 and 1.13 THz [19]. A substantial amount of research has been undertaken in antenna design to generate multiband frequencies in the millimeter and terahertz regions, utilizing particular materials appropriate for high-frequency applications while maintaining minimal antenna dimensions. Recent investigations on multiband antennas functioning at microwave frequencies have been constrained, however they are in high demand due to their applicability across numerous domains. The design of the microstrip antenna has been carried out in [20] and can work in 3 frequency bands, namely 23.9 GHz, 35.5 GHz and 70.9 GHz. A meanderline antenna integrated with a shorting pin can produce multiband frequencies at 2.2 GHz, 3.5 GHz, 4.2 GHz, 4.95 GHz, and 5.6 GHz. However, the meanderline structure and the presence of external components make the design somewhat more complex.

A meanderline antenna integrated with a shorting pin can produce multiband frequencies at 2.2 GHz, 3.5 GHz, 4.2 GHz, 4.95 GHz, and 5.6 GHz [21]. Nevertheless, the design is more complicated as a result of the meanderline structure. Microstrip patch antennas using Defected Ground Structure and reconfigurable techniques have been developed to achieve multiband frequency distribution. However, the additional external components complicate the design [22].

Consequently, this investigation suggests the study performance of the log-periodic antenna for multiband applications. Five LPA models with different patch geometries are designed and compared in terms of reflection coefficient, surface current distribution, radiation pattern, and directivity. We also compare simulation and measurement results. The main contributions of this paper are:

- Five different LPA models with patch shape variations are designed to determine the differences in the number of frequency resonances that occur at frequencies of 3-11 GHz. The basic patch antenna is rectangular in shape, which is modified to form 5 different models, namely U shape (model 1), S shape (Model 2), O shape (Model 3), full rectangular shape (Model 4), and rhombic shape (Model 5).
- The performance of the five antenna models is compared with previous references to determine which model produces the highest number of resonance frequencies and the best minimum S11 performance, as well as directivity and antenna application performance.

2. ANTENNA DESIGN

The proposed log-periodic microstrip antennas are fabricated on a Rogers RO4003C substrate with a thickness of 0.8 mm, a relative permittivity of $\varepsilon r = 3.55$, and a copper layer thickness of 0.035 mm. The substrate dimensions are 173×70 mm. Five antennas equipped with square-patch radiators, designated as LPA Model 1 through Model 5, are examined. All models utilize the same double-substrate configuration, featuring feeding width (fw) of a 3-mm-wide 50-Ω microstrip input line positioned along the center of the upper substrate. The ground plane and microstrip line are depicted in Fig. 1, while Fig. 2 illustrates the various radiator patch geometries employed in Models 1–5. We designed five different radiator shapes that are basically rectangular. Model 1 is a rectangular shape that resembles the letter

U (as shown in Fig 2a), Model 2 possesses the letter S (as shown in Fig 2b), The Model 3 corresponds to the letter O (as seen in Fig 2c), Model 4 is a full rectangular shape (as revealed in Fig 2d) and Model 5 is a square shape like a rhombus(as illustrated in Fig 2e). All models are composed of 15 elements ranging from small to large in size with a graduated size. All structures are modeled within the frequency range of 3 to 11 GHz and are optimized to achieve multiband operation, with |S11| less than -10 dB at multiple discrete frequency bands. All simulations were performed utilizing CST Studio Suite with open (radiation) boundary conditions and a discrete frequency scan ranging from 3 to 11 GHz.

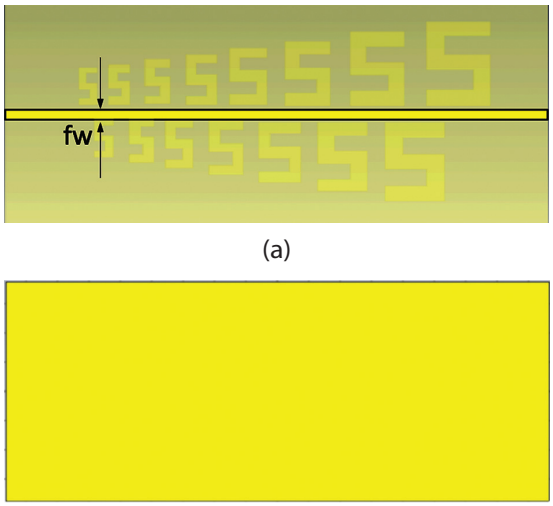

(a)

(b)

Fig. 1. Back and middle view: (**a**) transmission line between two substrate, (**b**) ground plane of antenna

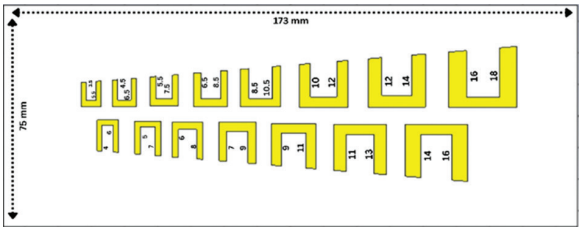

(a)

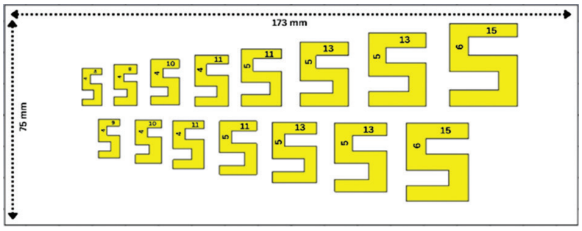

(b)

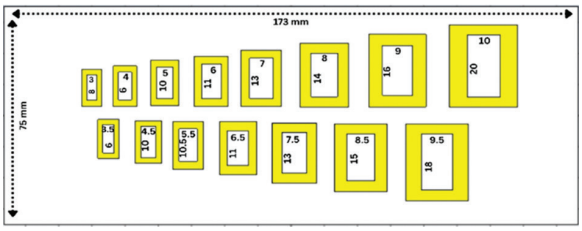

(c)

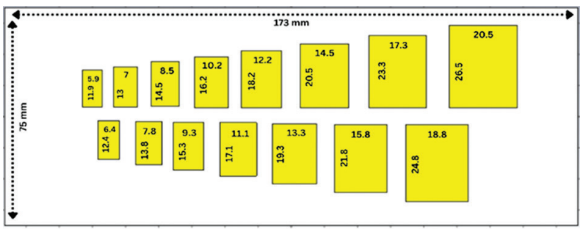

(d)

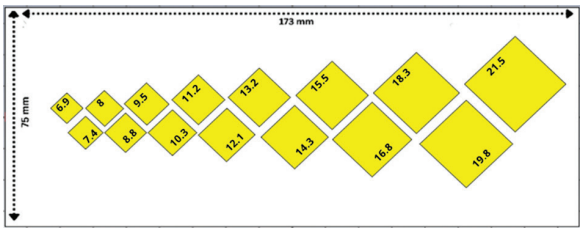

(e)

Fig. 2. Log Periodic Antenna geometries: (**a**) Model 1, (**b**) Model 2, (**c**) Model 3, (**d**) Model 4, (**e**) Model 5

3. RESULTS

The multiband behavior of antenna structures arises from the sequential activation of radiators of varying dimensions as the frequency escalates. Log Periodic Antennas can generate multiband capabilities due to their physical configuration, which comprises several dipole elements of differing lengths. The signal will traverse the small components at the front and be received by the elongated components at the rear. The segment of the antenna responsible for receiving this signal is termed the active region. This active region will oscillate along the antenna shaft based on the frequency of the received signal. Each component of a Log Periodic antenna is precisely dimensioned to resonate at a certain frequency, adhering to the half-wave formula ($\lambda/2$). The rearmost (longest) element establishes the minimum frequency limit that can be received. The foremost part establishes the maximum frequency limit that can be received. The central element occupies the frequency void. Log Periodic Antennas are multiband and broadband due to their design, which incorporates elements that correspond to each frequency throughout their length, enabling signal resonance.

From the simulation results, the antenna reflection coefficient performance can be seen in Fig. 3, namely S_{11} of LPA (a) Model 1, (b) Model 2, (c) Model 3, (d) Model 4, and (e) Model 5. From the simulation results, the reflection coefficient performance in different multibands is obtained. Model 1 produces 4 multiband frequencies (at 3 GHz, 4.3 GHz, 6.27 GHz, and 6.78 GHz) with a minimum reflection coefficient value of -21.21 dB at 3 GHz. Model 2 has 7 multiband frequencies at 3 GHz, 4.5 GHz, 6 GHz, 6.79 GHz, 7.62 GHz, 8.71 GHz, and 9.12 GHz with a minimum S11 of -25.8 dB at 4.5 GHz. The 3 GHz frequency can be used for Wi-Fi, LTE, radar, and satellite communications, while the 4.5 GHz frequency can be used for Wi-Fi, radar, and military communications.

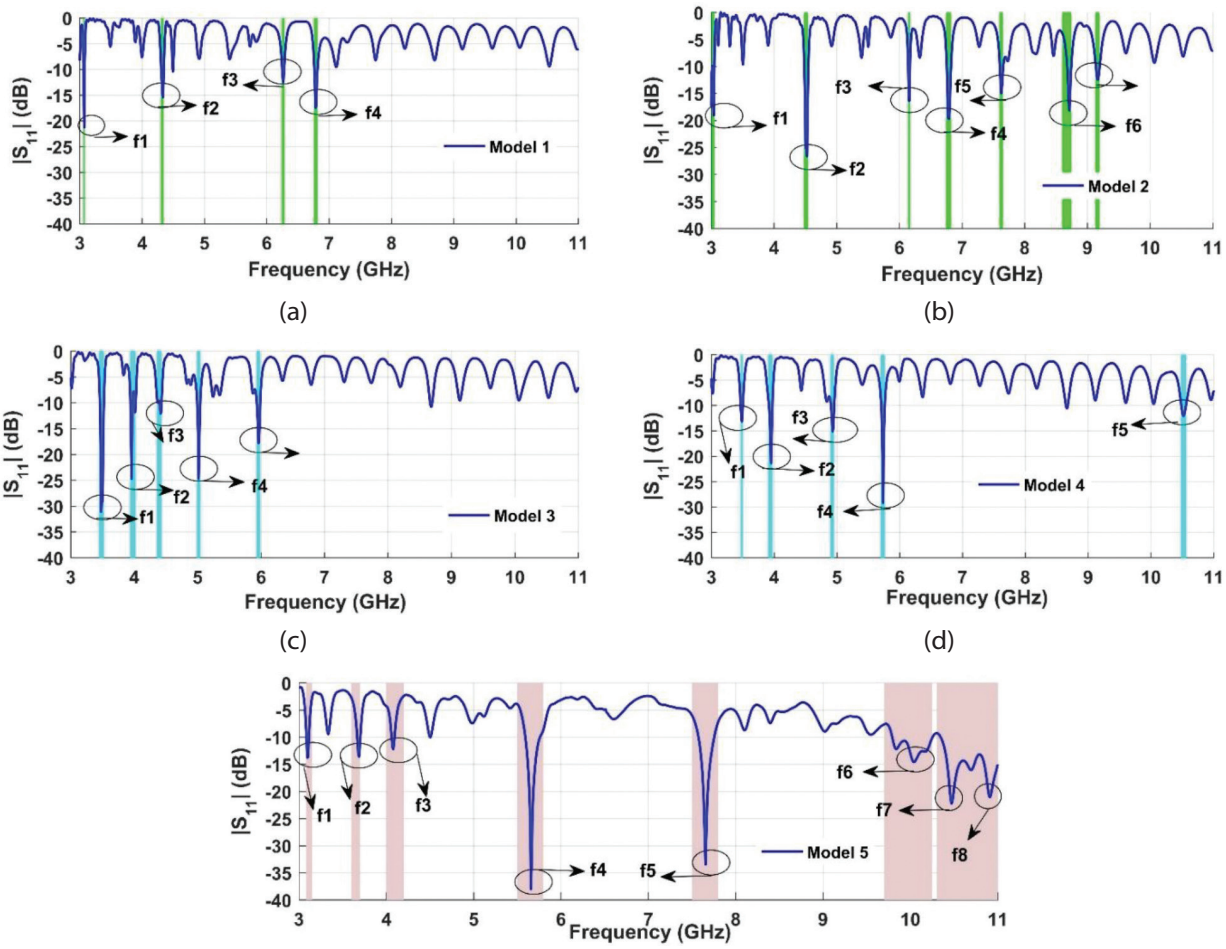

Fig. 3. S_{11} performance of LPA: (a) Model 1, (b) Model 2, (c) Model 3, (c). Model 4 and (e) Model 5

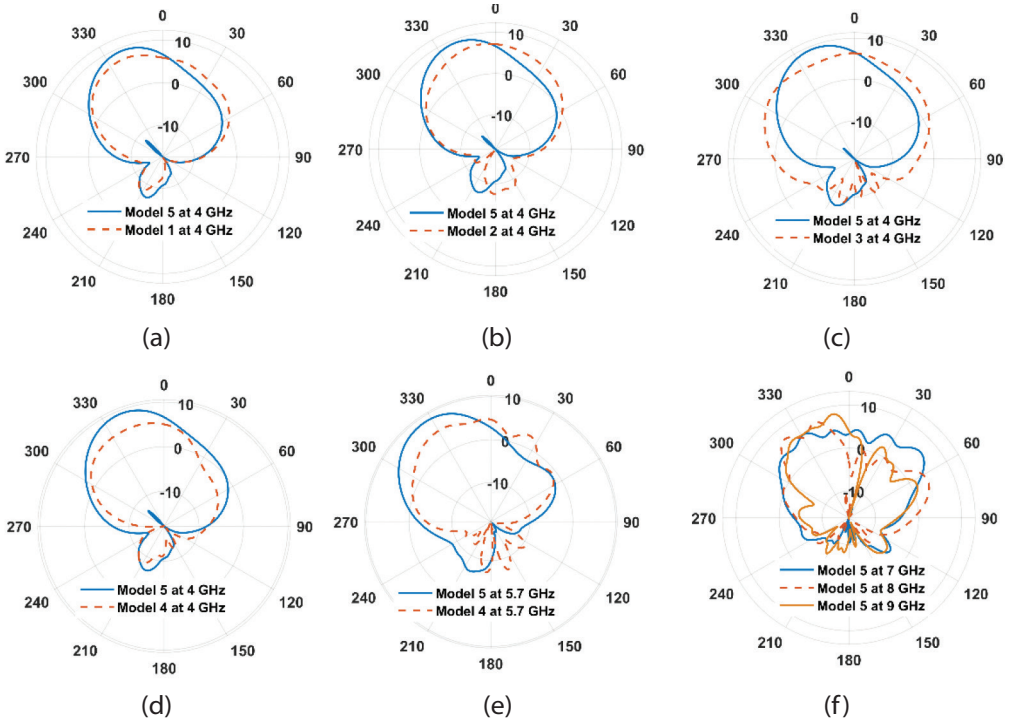

Fig. 4. Radiation pattern Polar plot at *Phi*=0° of LPA: (**a**) model 5 compared to model 1 at 4 GHz, (**b**) model 5 compared to model 2 at 4 GHz, (**c**) model 5 compared to model 3 at 4 GHz, (**d**) model 5 compared to model 4 at 4 GHz, and (**e**) model 5 compared to model 4 at 5.7 GHz,and model 5 at frequency: 7,8,9 GHz

Model 3 has 5 resonance frequencies at 3.48 GHz, 3.96 GHz, 4.4 GHz, 5 GHz and 5.97 GHz with a minimum reflection coefficient of -31.16 dB at 3.48 GHz, Model 4 has resonance frequencies in 5 bands (with S11 < -10 dB at 3.48 GHz, 3.95 GHz, 4.93 GHz, 5.73 GHz and 10.51 GHz) and has a minimum S11 at a frequency of 5.73GHz of -28.9 dB.

The 3.48 GHz frequency can be used for Wi-Fi 6, Fixed Wireless Access (FWA), and IoT due to its high speed, low latency, and stable connectivity on mobile devices. However, Model 5 has 8 multiband frequencies that have a minimum reflection coefficient of -37.86 dB at a frequency of 5.7 GHz. However, Model 5 has 8 multiband frequencies at 2.4 GHz, 3 GHz, 3.7 GHz, 5.7 GHz, 7.6 GHz, 10 GHz, 10.5 GHz, and 10.9 GHz. Model 5 has the minimum reflection coefficient of -37.86 dB at a frequency of 5.7 GHz. The 5.7 GHz frequency can be used for communication, surveying, surveillance, and radar on UAVs and airborne. It has high resolution in tracking objects, has good penetration detection capabilities, and is more stable in various weather conditions.

Fig. 4 shows comparison of radiation polarization in the form of polar plots of several model forms against model 5. We elected to demonstrate the radiation pattern comparison in Fig. 4 (a) - (d) at 4 GHz since this is the frequency at which the Model 5 reaches the highest level of mainlobe magnitude. At 4 GHz frequency, models 1 and 2 have mainlobe magnitude of 7.29 dBi and 7.31 dBi. While the mainlobe direction of Model 1 and Model 2 is 210 and 80. Side Lobe Level (SLL) of Model 1 and Model 2 at 4 GHz frequency is -15.4 dB and -14.8 dB. At 4 GHz frequency, Mainlobe magnitude of Model 3 is 6.35 dBi, with main lobe direction 20, angular width 117.50, and SLL -14.5 dB. While, model 4 has a main lobe magnitude of 5.56 dBi with mainlobe direction 140 and SLL -13.7 dB. At 4 GHz, LPA Model 5 produces a mainlobe 9.21 dBi, with mainlobe direction 210, angular width 46.60, and -16.3 dB. At 4 GHz, Model 5 has the best mainlobe directivity and SLL compared to the other models of -16.3 dB. However, Model 3 has the best mainlobe direction, which is 20. This indicates that the direction of the mainlobe is only slightly shifted from the center. Fig. 4 (e) is a comparison of the radiation pattern in the form of LPA polar plot at a frequency of 5.7 GHz for LPA Model 5 and Model 4. It can be seen from the figure that by making a rhombus-shaped radiator (Model 5) can increase the mainlobe by 3.34 dBi compared to a rectangular radiator (Model 4). Fig. 4 (f) depicts the radiation pattern of model 5 at frequencies of 7, 8, 9 GHz with mainlobe magnitudes of 6.37 dBi, 7.33 dBi and 8.16 dBi and mainlobe directions of 470, 390 and 90. While the SLL of Model 5 at these frequencies are -0.5, -3.3, and -6.2 dB, respectively. At a frequency of 7 GHz the radiation pattern performance of Model 5 decreases compared to frequencies of 4, and 5.7 GHz but increases at frequencies of 8 and 9 GHz. From Fig. 4 (f) it can also be seen that there is an increase in the performance of the main lobe direction and SLL of the model 5 antenna at frequencies of 7.8 and 9 GHz.

Fig. 5 illustrates the surface current distribution for each model. Surface current refers to the electric current flowing across the antenna surface.

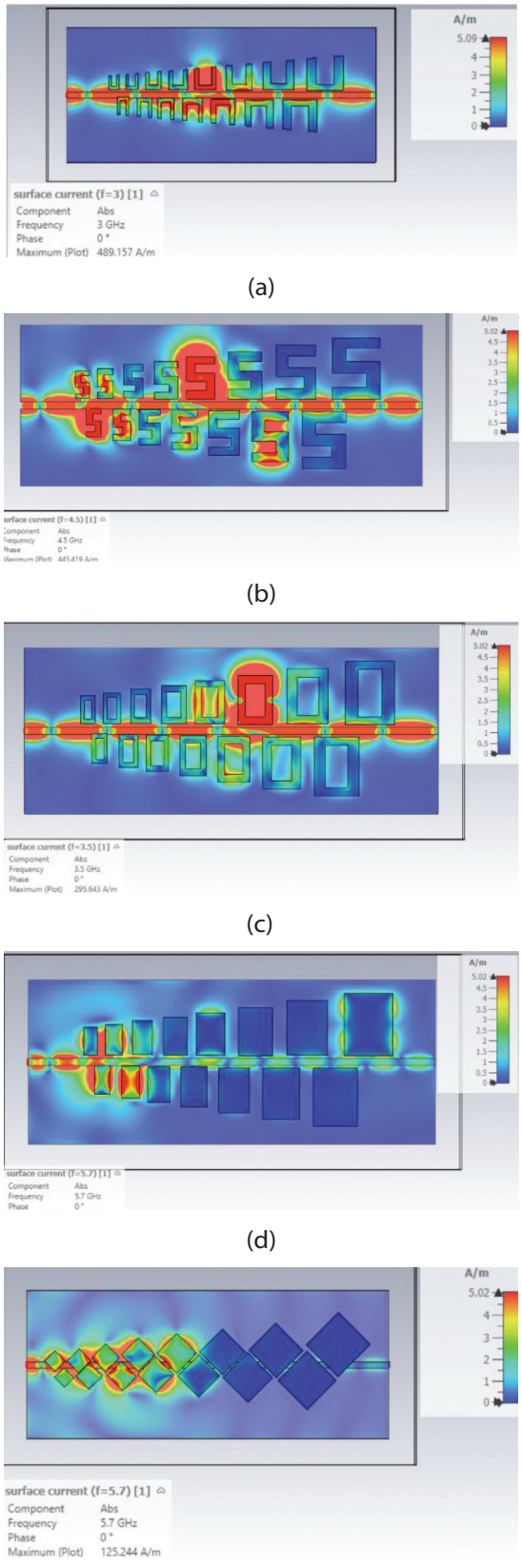

Fig. 5. Surface Current performance of LPA: (**a**) Model 1, (**b**) Model 2, (**c**) Model 3, (**d**). Model (4) and (**e**) Model 5

In this study, surface current was observed at different frequencies based on the minimum reflection coefficient of the antenna as discussed in the previous section. The surface current visualization shows varying colors representing intensity: blue (weak), green (moderate), yellow (strong), and red (very strong). Model 1 has the lowest reflection coefficient at 3 GHz and produces a surface current of 489.16 A/m. Model 2 (shaped like the letter S) produces a surface current of 445.4 A/m at 4.5 GHz, and Model 3 produces a surface current of 295.643 A/m at 3.5 GHz. Model 4 produces a surface current of 148.255 A/m at 5.7 GHz. While Model 5 produces a surface current of 125.244 A/m. Fig. 6 depicts the directivity performance vs frequency of LPA Model 1-5. From Fig. 6, it can be seen that LPA model 5 has greater directivity at most frequencies compared to other models at most frequencies, namely at 3 GHz, 4 GHz, 5.7 GHz, 6 GHz, 8 GHz, and 10 GHz. At a frequency of 5 GHz, Model 1 antenna has a directivity only slightly higher than Model 5, namely, the difference is only 0.71 dBi. At a frequency of 7 GHz, there is an increase in the directivity of model 2 compared to model 5 by 0.966 dBi. At a frequency of 11 GHz, antenna models 1, 2, and 3 have higher directivity than models 5 and model 4. However, the greatest directivity is located at a frequency of 4 GHz, obtained by Model 5 of 9.21 dBi.

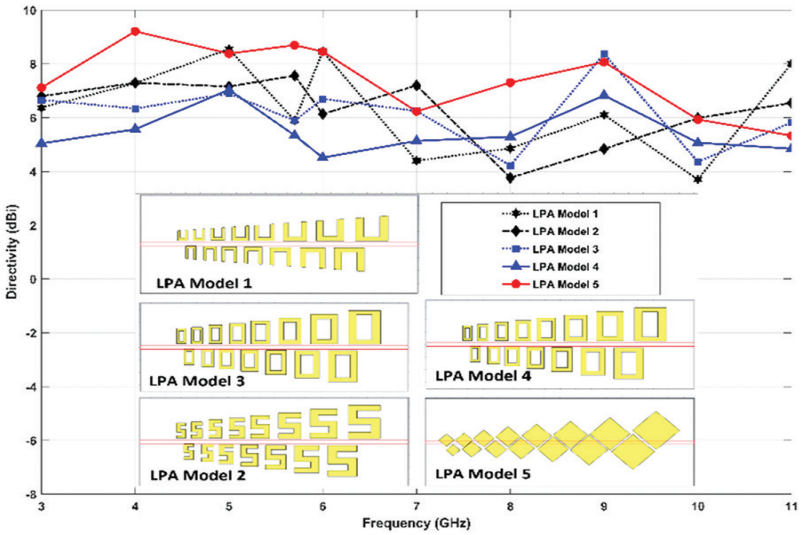

Fig. 6. LPA Directivity vs Frequency performance

At a frequency of 4 GHz, the Log Periodic Antenna Model 5 has a directivity of 9.21 dBi, while Model 4 has a directivity of 5.56 dBi. This shows an increase in directivity of 3.65 dBi by making the radiator rhombus-shaped. Meanwhile, at frequencies of 6 GHz and 8 GHz, Model 5 has an increase in gain of 3.86 dBi and 2 dBi, respectively. Differences in radiator shape and radiator dimensions can affect the formation of multi-band frequencies and affect the directivity performance of the antenna.

Fig. 7 shows a comparison of simulation and measurement results performance of S11 using a VNA. Antenna fabrication was performed on an LPA Model 5 using Rogers RO4003C material using a PCB etching process. Prior to measurements, the antenna power supply was connected to an SMA connector and measurements were taken using a calibrated VNA. It results show slight differences performance of S11 but they are similar at some frequencies. The measured results seem to be slightly better than the simulated results. These discrepancies are mainly attributed to fabrication tolerances in the substrate and etching, small variations in the dielectric properties, and additional mismatch and loss introduced by the SMA connector and soldering. Despite these effects, the measured |S11| remains below −10 dB at the main operating bands, confirming that the fabricated antenna operates as intended.

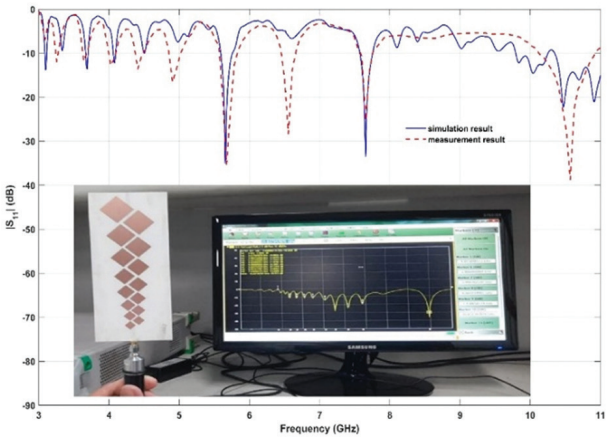

Fig. 7. Comparison of simulation and Measurement results

Table 1 shows a comparison of the antenna's performance against its corresponding reference. The antennas [23, 27, 28, 32] exhibit smaller dimensions and broader bandwidths across each frequency multiband relative to our developed antenna; nevertheless, our antenna features a greater number of multibands, superior maximum directivity, and enhanced impedance bandwidth (S11) compared to them. Antennas [24-26, 30-34] exhibit greater bandwidths over many

frequency multibands; however, they are bigger in size compared to our developed antenna, which features more frequency multibands and superior impedance bandwidth. Table 1 demonstrates that the dimensions of the model 5 antenna are less than those of models 1 through 4. Antenna 5 possesses a greater number of frequency multibands, superior impedance performance, and enhanced gain and efficiency compared to models 1 through 4. This concludes that the antenna can be recommended for multiband applications.

Table 1. Comparison of Related Studies

Ref	Antenna size Substrate	n	freq	Min S11 (dB)	Bandwidth	Max Dir & Max Eff	Application
[23]	0.034λ × 0.004 λ FR4	5	900, 1900, 2600, 5200, 5800	-23 (at 5.8 GHz)	25.3%, 49.6%, 34.8%	6.3 dBi n/a	GSM (880–960 MHz), DCS, PCS, UMTS, 2.4 GHz WLAN, WiMAX, 5 GHz WLAN (5725–5825 MHz)
[24]	0.18λ × 0.18 λ FR4	4	1.8, 2.8, 5.7, 9.6	-28.64 (at 5.7 GHz)	11%, 10.5%, 5.52%, 9.3%	3.1 dBi n/a	GNSS (1.6 GHz), WiMAX (2.5 GHz), WLAN (5.8 GHz), X-band (9.5 GHz)
[25]	0.14λ × 0.14 λ FR4	3	1.2, 3.9, 5.7	-14.7 (at 5.7 GHz)	6.72%, 4.3%, 2.44%	n/a	L-band (1.2 GHz), WLAN (5.7 GHz)
[26]	0.175 λ × 0.09 λ FR4	2	3.5, 5.8	-15 (at 5.8 GHz)	11,1%, 13,91%	13 dB 82%	5G Sub-6 GHz MIMO, LTE-U/LAA, Smartphone,Massive MIMO 10×10
[27]	0.048λ × 0.024λ FR4	7	1.2, 3.9, 5.7	-15 (at 5.7 GHz)	6.72%, 4.3%, 2.44%	3.78 dB 69.18%	GSM, GPS, Galileo, DCS, PCS, UMTS, LTE 2300/2500, WLAN, WiMAX, 5G sub-6 GHz
[28]	0.02λ × 0.02 λ FR4	5	2.4, 3.5, 4.4, 6.09, 7.7	-9 (at 6.6 GHz)	9.16%, 28.7%, 23.18%, 6.45%, 14.2%	2.92 dBi 94.8%	Bluetooth, WLAN 2.4 & 5.8 GHz, WiMAX, LTE, ITS 5.9 GHz, X-band comm
[29]	n/a FR4	3	2.4, 3.5, 5.7	-25 (at 5.7 GHz)	150 MHz, 324 MHz and 1608 MHz	4.33 dBi n/a	WBAN (Wireless Body Area Network), ISM 2.4 & 5.7 GHz, UWB 3.5 GHz
[30]	0.79λ × 0.79 λ RT Duroid 5880	3	5.7, 6, 6.45	-13 (at 5.7 GHz)	n/a	6.26 dBi n/a	WLAN 5 GHz, ISM 5.725–5.875 GHz, C-Band Comm, Triplexer Systems
[31]	0.84λ × 0.36 λ	4	1.8, 2.4, 3.6, 5.8	-20 (5.8 GHz)	18.97%, 54.84%, 10.78%	6.38 dBi 41%	NB-IoT/ISM/5 G
[32]	0.026λ × 0.035 λ FR408	5	3.71, 4.21, 5.16, 6.98, 9.44	-20 (at 5.16 GHz)	40 MHz,50 MHz, 110 MHz, 80 MHz. 70 MHz	5 dB 80%	Wireless Communication
[33]	0.35λ × 0.35 λ	6	2.33, 3.3, 5.03, 6.84, 8.12, 9.75	-20 (at 5.03 GHz)	4.72 %, 4.24 %, 3.38 %, 3.95 %, 3.94 %, and 6.67 %,	6.48 dBi n/a	5G/X Band
[34]	0.179λ × 0.086 λ FR4	2	3.7, 4.9	-27 (at 5 GHz)	5,4%, 4.08%	5 dBi 75%	MIMO 5G Communication
[35]	0.16λ × 0.08 λ FR4	2	3.5, 5.5	-24 (at 5.5 dB)	12,86%, 19.8%	3.2 dBi 78%	5G Smart Phone
Model 1	0.173λ × 0.055 λ RO4003	4	3, 4.3, 6.2, 6.8	-15.3 (4.3 GHz)	0.65%, 0.93%, 0.64%, 0.73%	8.55 dBi 52%	Wifi, 5 G, Radar (3GHz), FWA, IoT (4.3 GHz) and Wi-fi 6E and Industrial Appl.
Model 2	0.173λ × 0.055 λ RO4003	7	3, 4.5, 6,16, 6,79, 7.62, 8.71, 9.17	-15.95 (6.16GHz)	1.05%, 1.55%, 0.49%, 1.03%, 8.73%, 0.91%, 2.18%	7.3 dBi 30%	5G, Wifi (3GHz), Radar, Military communication (4.5 GHz, 7.6 GHz), Wifi 6E (6 GHz), Remote sensing (8.7 GHz), Navigation (9 GHz), UAV, Airborne Radar
Model 3	0.2λ × 0.064 λ RO4003	5	3.48, 3.96, 4.41, 5.01, 5.97	-17.62 (5.97)	1.72%, 2.13%, 1.6%, 2.02%, 0.5%	8.3 dBi 64%	5 G, FWA, IoT (3.5 GHz), Satellite communication, radar (4GHz), 5G (4.4GHz), Wifi, Radar (5 GHz), Wifi 6E and FWA (6GHz)
Model 4	0.2λ × 0.064 λ RO4003	5	3.48, 3.93, 5.73, 10.5	-29.4 (5.73)	0.95%, 1.37%, 1.22%, 1.05%, 0.76%	7.04 dBi, 60.4%	Wifi, 5 G, Radar (3GHz), Satellite Comm (4 GHz), Wifi, Radar (5 GHz), Remote sensing, UAV communication (10 GHz)
Our purposed (Model 5)	0.138λ × 0.044 λ RO4003	8	2.4, 3, 3.7, 5.7, 7.6, 7.6, 10, 10.5, 10.9	-38.03 (5.7)	0.41%, 0.96%, 0.81%,0.73%, 2.82%, 2.34%, 11.64%	9.2 dBi 84%	Wifi (2.4 GHz), 5 G, Radar (3GHz, 3.6 GHz), Satellite (4 GHz), Wifi, Radar (5 GHz), UAV communication (5.7 GHz), Airborne radar, remote sensing (9 and 10 GHz)

Table 1 shows a comparison of the antenna's performance against its corresponding reference. The antennas [23, 27, 28, 32] exhibit smaller dimensions and broader bandwidths across each frequency multiband relative to our developed antenna; nevertheless, our antenna features a greater number of multibands, superior maximum directivity, and enhanced impedance bandwidth (S11) compared to them. Antennas [24-26, 30-34] exhibit greater bandwidths over many frequency multibands; however, they are bigger in size compared to our developed antenna, which features more frequency multibands and superior impedance bandwidth. Table 1 demonstrates that the dimensions of the model 5 antenna are less than those of models 1 through 4. Antenna 5 possesses a greater number of frequency multibands, superior impedance performance, and enhanced gain and efficiency compared to models 1 through 4. This concludes that the antenna can be recommended for multiband applications.

4. CONCLUSION

This study presented a comparative analysis of five log-periodic microstrip antennas with different square-patch geometries designed to operate between 3 and 11 GHz. The simulations demonstrate that Model 1 creates four multiband frequencies, Model 2 produces seven, Model 3 produces five, Model 4 produces five, and Model 5 produces eight operational bands with $|S11|<-10$ dB. Model 5 produces 8 resonance frequencies at 2.4, 3, 3.7, 5.7, 7.6, 10, 10.5 and 10.9 GHz with the best impedance, minimum $|S11|$ of -37.86 dB at 5.7 GHz, and the highest directivity of 9.21 dBi at 4 GHz. Model 5 was fabricated and measured, and the measured S11 curve agrees reasonably well with the simulation. Compared with previously reported multiband antennas, the proposed Model-5 LPA offers more resonant bands, a minimum resonance frequency at 5.7 GHz, and higher directivity while keeping a simple, single-feed structure, making it suitable for multistandard communication and radar applications such as Wi Fi, 5G, UAV, and remote-sensing systems. Future work will focus on measuring radiation patterns and efficiency, further optimizing the radiator shapes, and integrating the proposed antenna into complete communication and radar front-ends.

REFERENCES

[1] K. Patel, F. Thakkar, "Design and Analysis of Miniaturized Dielectric Resonator Antenna with Ring DGS and Chord-Cut Ground Plane for Multiband Wireless Applications", International Journal of Microwave and Optical Technology, Vol. 20, No. 3, 2025, pp. 269-280.

[2] M. Al-Abbasi, T. A. Latef, "Wideband circularly polarized fractal antenna with SSRR metasurface for 5G applications", International Journal of Electrical and Computer Engineering Systems, Vol. 15, No. 1, 2024, pp. 89-98.

[3] G. M. Amrutha, T. Sudha, "Triple Band Antenna for 5G Applications", Proceedings of the International Conference on Advances in Computing, Communications and Informatics, Bangalore, India, 19-22 September 2018, pp. 1650-1652.

[4] A. K. Vallappil, B. A. Khawaja, A. M. Alenezi, "Miniaturized Ultra-Wide Band (UWB) Delta-Stub Based 4-Way Power Divider with Enhanced Isolation For Internet of Things (IoT) and Next-Generation Wireless Systems", International Journal of Electrical and Computer Engineering Systems, Vol. 15, No. 9, 2024, pp. 733-741.

[5] R. A. Firdaus et al. "Enhancing the Performance of Rectangular Microstrip Antenna with T-slot Addition for 5G Network Applications", International Journal of Microwave and Optical Technology, Vol. 20, No. 3, 2025, pp. 290-297.

[6] B. Xiao, H. Wong, K. L. Yeung, "Penta-band Dual-fed Smart Glasses IoT Antenna", Proceedings of the 14th European Conference on Antennas and Propagation, Copenhagen, Denmark, 15-20 March 2020, pp. 20-23.

[7] N. Nurhayati, A. M. De-Oliveira, W. Chaihongsa, B. E. Sukoco, A. K. Saleh, "A comparative study of some novel wideband tulip flower monopole antennas with modified patch and ground plane", Progress in Electromagnetics Research C, Vol. 112, 2021, pp. 239-250.

[8] N. Nurhayati et al. "Design and studies of monopole antenna integrated with metamaterial-based CSRR and rectangular spiral shaped for super wide band application", Results in Engineering, Vol. 26, 2025, p. 105459.

[9] K. Vinayagam, R. Natarajan, "Polarization Reconfigurable Patch Antenna Using Parasitic Elements for Sub-6 GHz Applications", International Journal of Electrical and Computer Engineering Systems, Vol. 16, No. 1, 2025, pp. 1-7.

[10] M. Garcia-Fernandez, Y. Alvarez-Lopez, F. Las Heras, "Evaluation of an unmanned aerial system for antenna diagnostics and characterization",

Proceedings of the 12th European Conference on Antennas and Propagation, London, UK, 9-13 April 2018.

[11] M. G. Fernandez, G. A. Narciandi, A. Arboleya, C. V. Antuna, F. L. H. Andres, Y. A. Lopez, "Development of an Airborne-Based GPR System for Landmine and IED Detection: Antenna Analysis and Intercomparison", IEEE Access, Vol. 9, 2021, pp. 127382-127396.

[12] I. V. Trivino, A. K. Skrivervik, "Enhancing the beamwidth of low profile single-fed microstrip antennas using parasitic elements", Proceedings of the 16th European Conference on Antennas and Propagation, Madrid, Spain, 27 March - 1 April 2022.

[13] M. García-Fernández, Y. A. López, F. Las-Heras Andrés, "Airborne multi-channel ground penetrating radar for improvised explosive devices and landmine detection", IEEE Access, Vol. 8, 2020, pp. 165927-165943.

[14] W. J. Krzysztofik, "Fractal geometry in electromagnetics applications - from antenna to metamaterials", Microwave Review, Vol. 19, No. 2, 2013, pp. 3-14.

[15] P. Natarajan, T. Sigamani, "Design implementation analysis of multi-band antenna for terrestrial applications", Heliyon, Vol. 10, No. 18, 2024, p. e37519.

[16] A. Youssef, I. Halkhams, R. El Alami, M. O. Jamil, H. Qjidaa, "Innovative flexible and compact patch antenna for multiband terahertz applications", Scientific African, Vol. 24, 2024, p. e02196.

[17] Y. Amraoui, I. Halkhams, R. El Alami, M. O. Jamil, H. Qjidaa, "High gain MIMO antenna with multiband characterization for terahertz applications", Scientific African, Vol. 26, 2024, p. e02380.

[18] Y. Amraoui, I. Halkhams, R. El, M. Ouazzani, H. Qjidaa, "Terahertz dual-band antenna design with improved performances using FSS-based metasurface concept for wireless applications", Scientific African, Vol. 27, 2025, p. e02566.

[19] A. Youssef, I. Halkhams, R. El Alami, M. O. Jamil, H. Qjidaa, "A new approach to designing a multiband antenna using photonic crystals and load graphene for terahertz application", Results in Engineering, Vol. 22, 2024, p. 102327.

[20] S. Punith, S. K. Praveenkumar, A. A. Jugale, M. R. Ahmed, "A Novel Multiband Microstrip Patch Antenna for 5G Communications", Procedia Computer Science, Vol. 171, 2020, pp. 2080-2086.

[21] J. O. Abolade, D. B. O. Konditi, "A shorting-pin based compact meander multiband printed monopole antenna", Heliyon, Vol. 7, No. 11, 2021, p. e08390.

[22] A. Tiwari, G. K. Soni, D. Yadav, S. V. Yadav, M. V. Yadav, "Rectangular loaded ring shaped multiband frequency reconfigurable defected ground structure antenna for wireless communication applications", Results in Engineering, Vol. 25, 2025, p. 104339.

[23] Y. C. Lee, J. S. Sun, "A new printed antenna for multiband wireless applications", IEEE Antennas and Wireless Propagation Letters, Vol. 8, 2009, pp. 402-405.

[24] T. Ali, M. M. Khaleeq, R. C. Biradar, "A multiband reconfigurable slot antenna for wireless applications", AEU - International Journal of Electronics and Communications, Vol. 84, 2018, pp. 273-280.

[25] K. D. Prasad, T. Ali, R. C. Biradar, "A compact slotted multiband antenna for L-band and WLAN applications", Proceedings of the 2nd IEEE International Conference on Recent Trends in Electronics, Information & Communication Technology, Bangalore, India, 19-20 May 2017, pp. 820-823.

[26] Y. Li, C. Y. D. Sim, Y. Luo, G. Yang, "Multiband 10-Antenna Array for Sub-6 GHz MIMO Applications in 5-G Smartphones", IEEE Access, Vol. 6, 2018, pp. 28041-28053.

[27] A. J. Khalilabadi, A. Zadehgol, "Multiband antenna for wireless applications including GSM/UMTS/LTE and 5G bands", Proceedings of the International Applied Computational Electromagnetics Society Symposium, Denver, CO, USA, 25-29 March 2018, pp. 10-11.

[28] F. Fertas, M. Challal, K. Fertas, "Miniaturized quintuple band antenna for multiband applications", Progress in Electromagnetics Research M, Vol. 89, 2020, pp. 83-92.

[29] H. Kaschel, C. Ahumada, "Design of a triband antenna microstrip for 2.4 GHz, 3.5 GHz and 5.7 GHz applied a WBAN", Proceedings of the Chilean Conference on Electrical, Electronics Engineering, Information and Communication Technologies, Pucon, Chile, 18-20 October 2017, pp. 1-7.

[30] A. Vala, A. Patel, "A multi-band SIW based antenna for wireless communication", International Journal of Electronics Letters, Vol. 9, No. 2, 2021, pp. 203-211.

[31] D. Kumar, D. Sharma, R. N. Tiwari, I. A. Khan, P. Kumar, "Multiband flexible MIMO antenna for NB-IoT/ISM/5 G and wearable applications", Results in Engineering, Vol. 27, 2025, p. 106088.

[32] I. J. Rajmohan, M. I. Hussein, "A compact multiband planar antenna using modified L-shape resonator slots", Heliyon, Vol. 6, No. 10, 2020, p. e05288.

[33] H. Kisioglu, "Multiband antenna design with a defected ground structure for 5G and X-band applications", International Journal of Electronics Letters, Vol. 190, 2025.

[34] C. Zhang et al. "A Dual-Band Eight-Element MIMO Antenna Array for Future Ultrathin Mobile Terminals", Micromachines, Vol. 13, No. 8, 2022, p. 1267.

[35] A. Khan, A. Wakeel, L. Qu, Z. Zahid, " Dual-band 8 × 8 MIMO antenna with enhanced isolation and efficiency for 5G smartphone applications", AEU - International Journal of Electronics and Communications, Vol. 163, 2023, p. 154600.